

TARGET DETECTION AND IDENTIFICATION USING ULTRA-WIDEBAND/SHORT-PULSE RADARS

K.M. Chen, E. Rothwell, D.P. Nyquist, P. Ilavarasan
J. Ross, Q. Li, C.Y. Tsai, R. Bebermeyer and A. Norman

Department of Electrical Engineering
Michigan State University
East Lansing, MI 48824

In this paper we will describe research activities at Michigan State University on target detection in a sea clutter environment and the identification of airborne targets using Ultra-Wideband/Short-Pulse (UWB/SP) radars.

Radar detection of a target flying above the sea surface is difficult when the sea clutter overwhelms the target response. The use of a UWB/SP radar combined with the following two techniques may help solve the problem. The first technique is to use a frequency-domain E-pulse to digitally filter out the sea clutter from the total received response without reducing the target response. This post-reception technique is possible because the sea clutter can be considered as the collection of specular reflections of the interrogating pulse from the ocean wave crests. The second technique involves waveform shaping of the interrogating pulse in such a way that when it illuminates the sea surface, the received sea clutter is basically canceled while the target response is not reduced. This pre-reception technique is based on sea surface periodicity -- the sea clutter can be represented by a sum of several damped sinusoids. The optimally synthesized waveform is called the clutter reducing transmit waveform. To study these target detection techniques, we have developed theoretical models of the sea clutter created by a short pulse incident on sinusoidal conducting sea surfaces of finite and infinite dimensions. We also conducted a series of measurements of scattering of a short pulse from a scaled sea surface model to verify the theory.

The identification of airborne targets can be improved by taking advantage of the good resolution of the UWB/SP radar. However, the early-time response of the target is strongly aspect-dependent. Thus, effective schemes are needed to solve this problem. To understand the nature of the target response to a short pulse, we have conducted a series of experiments to measure the pulse responses of scaled target models at an interval of 0.15° aspect angle in an anechoic scattering range using the frequency sweeping method. To identify a target based on its early-time response to a short pulse, we have developed a time-domain E-pulse technique to discriminate the target. We have also used neural network techniques to identify targets over a finite aspect angle range of about 10° . We found that the exponential correlation associative memory method is most effective. In the analysis of the early-time response of the target, it was found that the wavelet transformation can be used to effectively compress data.

RADAR IDENTIFICATION AND DETECTION USING ULTRA-WIDEBAND/SHORT-PULSE RADARS

K.M. Chen, E. Rothwell, D. P. Nyquist, J. Ross, P. Ilavarasan,
R. Bebermeyer, Q. Li, C. Y. Tsai, and A. Norman

Department of Electrical Engineering
Michigan State University
East Lansing, MI 48824

INTRODUCTION

An ultra-wideband/short-pulse (UWB/SP) radar has promising potential for target identification due to its ultra-high resolution capability and for target detection due to its clutter-suppression capability. This paper describes various research topics studied at Michigan State University on target identification and detection using a UWB/SP radar.

First the measurement of transient responses of airplane models illuminated by a short EM pulse is described. Then target identification schemes using these primarily early-time target responses are discussed. These target ID schemes include a time-domain imaging technique, a wavelet-transform technique and a neural network technique. Finally, schemes for detecting a target in a severe sea clutter environment using the E-Pulse technique or using the relative motion of the target are presented.

MEASUREMENT OF SHORT-PULSE TARGET RESPONSES

Michigan State University has a ground-screen-based time-domain scattering range and a free-field, anechoic chamber scattering range. The latter is used to measure high-resolution, early time responses of airplane models illuminated by a short EM pulse (about 60 ps width) which is synthesized from swept frequency measurements in the range of 2 to 18 GHz. A computer-controlled rotatable target positioner is capable of orienting the target to a precision of 0.15° in aspect angle. The data acquisition procedure is fully computer controlled, with the system transfer function deconvolved using a metallic sphere as a known calibration target. A typical set of synthesized target pulse responses is given in Figure 1, which shows the transient response of a 1:48 scale model B-58 (63 cm from nose to tail, and 36 cm from wing-tip to wing-tip) for aspect angles between 0 to 90 degrees, stepped in a 0.45° increment.

Using these measured target pulse responses, several schemes for target identification have been developed. These include the E-Pulse technique^{1,2}, a correlation scheme³, a time-domain imaging technique, a wavelet transform technique and a neural network technique. The latter three are described in this paper.

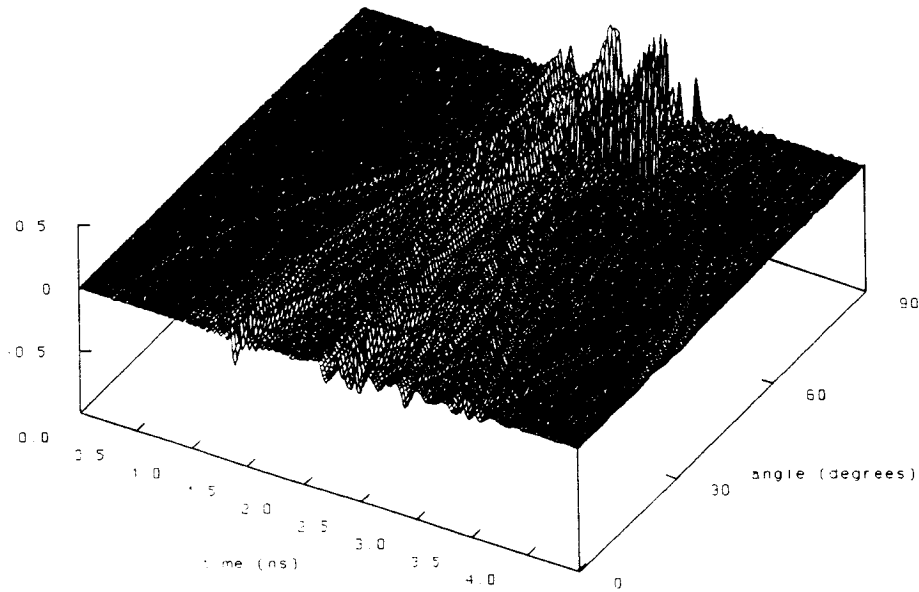


Figure 1. Transient response of 1:48 scale B-58 aircraft

TIME-DOMAIN IMAGING TECHNIQUE FOR TARGET IDENTIFICATION

The short-pulse response of a radar target provides significant information about the positions and strengths of scattering centers. If observations are made over a wide range of aspect angles, sufficient information is gained to obtain an image of the target.

Bojarski⁴ proposed a simple inverse scattering identity based on the physical optics approximation. He showed that the characteristic function of a conducting scatterer (which is unity within the target geometry and zero elsewhere) is given by the three-dimensional inverse Fourier transform of the scattered field as a function of the incident plane-wave wave vector \vec{k}^i . If scattered field information is only available within a plane, then the two-dimensional inverse transform yields the thickness of the scatterer as a function of position in that plane.

In the MSU free-field scattering range, aspect angle variation is obtained by target rotation. It is thus convenient to write the inverse scattering identity in polar coordinates. The thickness is then shown to be proportional to the function

$$T_{\omega}(\vec{\rho}) = \text{Re} \left\{ \int_{\phi_i=0}^{2\pi} \int_{K_0=0}^{\infty} E^s(K_0, \phi_i) e^{-jK_0 \rho \cos(\phi - \phi_i)} \frac{dK_0}{K_0} d\phi_i \right\} \quad (1)$$

where $\vec{\rho}$ is the position vector in the plane of the measurements, ϕ_i is the plane wave incidence angle, E^s is the back-scattered field measured at frequency ω and aspect angle ϕ_i , and $K_0 = 2k_0 = 2\omega/c$. By performing the integral over K_0 and recognizing this as the temporal inverse transform, the thickness function is proportional to

$$T_r(\vec{\rho}) = \int_0^{2\pi} r \left(-\frac{2\rho}{c} \cos(\phi - \phi_i), \phi_i \right) d\phi_i \quad (2)$$

where $r(t)$ is the time-integral of the inverse transform of E^s , i.e. the ramp response of the target. This time-domain physical optics inverse scattering identity has a very clear physical interpretation. The quantity $-2\rho \cos(\phi - \phi_i)/c$ is the two way transit time from the origin of coordinates to the point (ρ, ϕ)

along a plane wave incident at angle ϕ_i . Thus, the integral (2) is the sum over all aspect angles of the ramp response value corresponding to scattering from the point (ρ, ϕ) .

It is possible to enhance the edges of the image by merely using the impulse response (inverse transform of E^s) rather than the ramp response, since this corresponds to a derivative of the thickness response. This has been done in the examples shown in Figure 2. A distinct image of each target results, with the edges of the fuselage, wings, etc., being clearly displayed. Note that the physical optics approximation does not accommodate the shadowed regions, and thus hidden edges such as the rear of the forward wings are not strongly present.

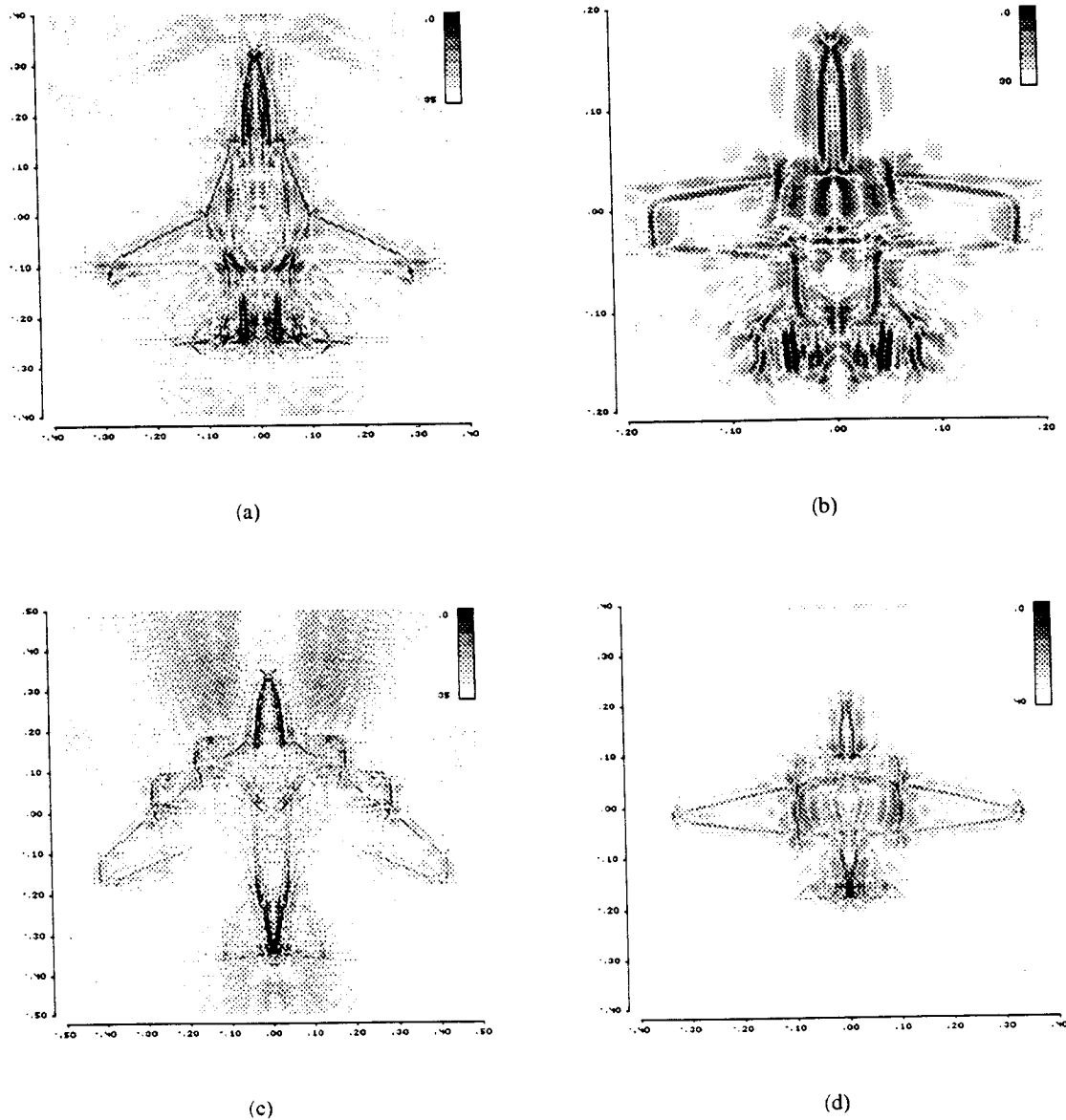


FIGURE 2. Images of aircraft found using time-domain, physical optics inverse scattering identity. Temporal waveforms synthesized from 2-18 GHz ultra-wideband responses, measured at 201 aspect angles between 0° (nose-on) and 180° . Information from unlit side supplied by symmetry. Axes are scaled to physical size in m, gray scale is in dB. (a) F-16 (1:32 scale), (b) A-10 (1:48), (c) B-52 (1:72), (d) TR-1 (1:48).

WAVELET-TRANSFORM TECHNIQUES FOR TARGET IDENTIFICATION

The sparse nature of the discrete wavelet transform (DWT) of SP scattering signals allows for a significant reduction in the storage of early-time signals. The DWT provides a linear transformation of a discretized signal into the "wavelet domain" much in the same manner as the discrete Fourier transform⁵. The signal is represented as a linear combination of wavelet basis

functions (analogous to sinusoids for the Fourier transform) and can thus be reconstructed by

$$s_i = \sum_{j=1}^N a_j w_{ij} \quad 1 \leq i \leq N \quad (3)$$

Here s_i is the signal sampled at time t_i , a_j is the amplitude of the j^{th} wavelet basis function, w_{ij} is the j^{th} wavelet basis function sampled at time t_i , and N is the length of the signal (usually a power of 2). Wavelet basis functions are constructed so that the wavelet coefficient vector $\{a_j\}$ is sparse for a certain class of waveforms (polynomials of a chosen degree). Because of this sparseness, the DWT can be used to compress the signal.

As an example, consider the nose-on (0°) response of a 1:72 scale B-52 sampled at 256 time points, as shown in Figure 3. Figure 4 shows the wavelet spectrum $\{a_j\}$ computed using a 256-point Lemarie DWT⁵. It is readily seen that only a small subset of the wavelet coefficients are significant. Note that the small values of coefficients a_{129} through a_{256} is due to an oversampling of the data by a factor of about 2. The DWT thus automatically compensates for frequency oversampling.

To see the effects of random noise on the wavelet reconstruction of data, zero-mean white Gaussian noise has been added to the nose-on response of the B-52, resulting in a waveform with a signal-to-noise ratio (SNR) of 10 dB. Figure 4 shows the wavelet spectrum of the noisy response. Although there is a perturbation of each of the wavelet coefficients, the values of the larger coefficients are changed only slightly. Thus, when only a few coefficients are retained in reconstructing the response, the result is a much more faithful representation than the original noisy waveform, as seen in Figure 3. In other words, much of the noise is represented by perturbation of very small wavelet coefficients which are neglected (effectively filtered out) in the reconstruction.

To provide an example of target identification using wavelet-stored data, the SP responses of five aircraft models -- B-52 (1:72 scale), B-58 (1:48), TR-1 (1:48), F-14 (1:48) and Mig-29 (1:48) -- were synthesized from frequency-domain measurements at 68 angles between 0° and 30° . The resulting signals were transformed using a 512 point Lemarie DWT and the spectra truncated to the largest 32 components. An identification scenario assumes that the 18° B-52 response arises from an unknown target. The measured response of the B-52 is correlated with the responses of all the other targets, at all aspects, reconstructed from their stored, truncated wavelet spectra. The result, shown in Figure 5, provides a correct identification, since the largest correlated output arises from the B-52. Also note that the target can be correctly identified over about a 3° range of angles. This gives a measure of the necessary aspect angle discretization needed when storing target SP signatures.

Finally, Figure 6 shows that contaminating the measured target signal with random noise at an SNR of 10 dB does not significantly reduce the identification capabilities of this technique.

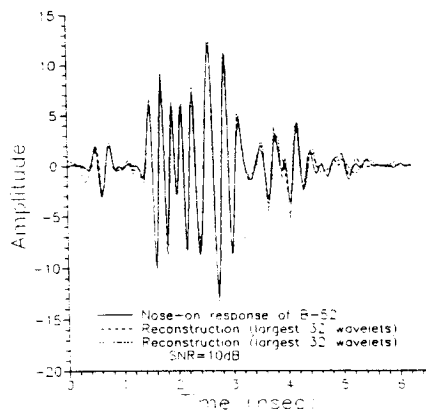


Figure 3. Nose-on (0°) response of B-52 aircraft model and 32 wavelet reconstruction.

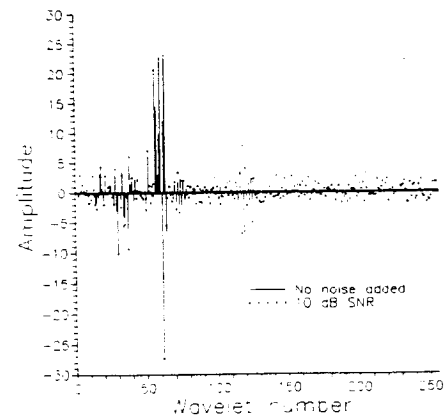


Figure 4. Wavelet spectrum of nose-on (0°) response of B-52 aircraft model.

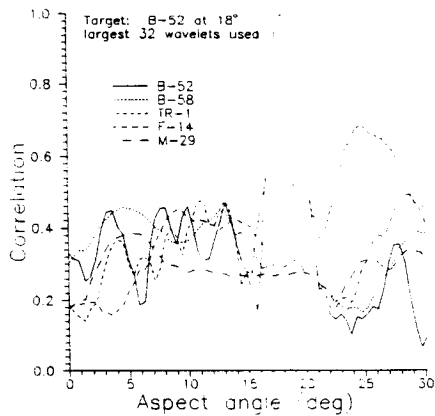


Figure 5. Maximum correlation of 18° B-52 response with responses from all targets. Target waveforms represented using 32 wavelets.

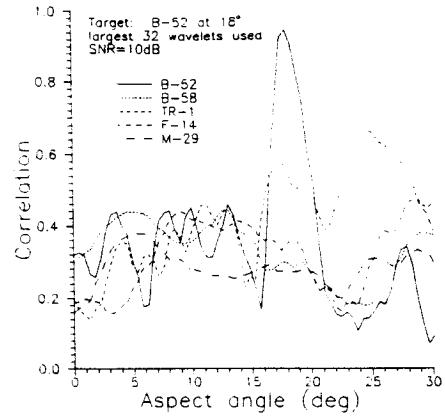


Figure 6. Maximum correlation of 18° B-52 noisy response with responses from all targets. Target waveforms represented using 32 wavelets. SNR=10 dB.

NEURAL NETWORK TECHNIQUES FOR TARGET IDENTIFICATION

Neural networks have great potential for storing and retrieving the large number of target signatures needed to perform aspect-dependent target identification (i.e., identification based on the early-time SP response). A number of neural network architectures for target identification were simulated, including feed-forward networks trained using back-propagation, and Hopfield networks. Particularly good success was observed with correlation associative memories, including generalized inverse networks (GI), exponential correlation associative memory networks (ECAM), and cascades of these networks (ECAM-GI). The wavelet transform technique described in the previous section has also been employed to reduce network size.

As an example, Figure 7 shows simulation results for the ECAM-GI cascaded network, designed to recognize three aircraft (F-14, B-58 and B-52) each at 19 different aspect angles between 0° and 90°. The results show that for low noise conditions, each of the 57 responses is correctly recognized. In fact, accurate identification is possible at noise levels of 0 dB SNR.

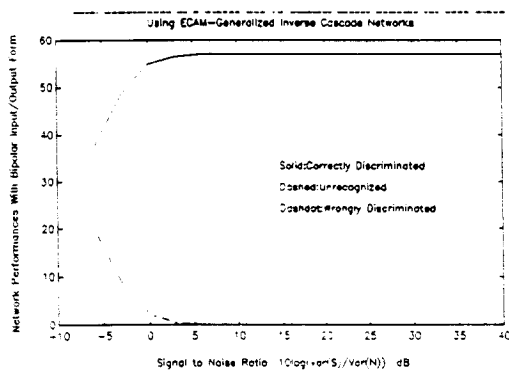


Figure 7. Overall performance of ECAM-GI cascade network, designed to recognize 3 aircraft at 19 aspect angles each.

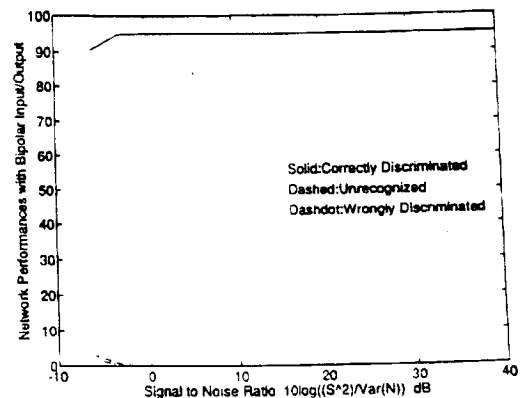


Figure 8. Performance of RDM-GI cascaded networks trained to recognize five target models each at 19 aspect angles. Analog inputs used.

More sophisticated networks are also being investigated, including recurrent dynamic correlation associative memory networks^{6,7} (RDM). The performance of a network using the RDM technique cascaded with the Generalized-Inverse method (RDM-GI) with fixed analog input is shown in Figure 8. This network was trained to recognize five targets (B-52, B-58, F-14, Mig-29, TR-1), each at 19 different aspect angles. Superior performance is seen in these figures, with better than 95% correct identification at SNR levels as low as -5 dB.

DETECTION OF TARGETS IN A SEA CLUTTER ENVIRONMENT USING UWB/SP RADAR

The detection of radar targets near the sea surface using transient signals is made difficult by the presence of a strong clutter return from the disturbed sea. However, if the scattering from water wave crests is primarily specular within the band of the interrogating signal, the E-pulse resonance cancellation technique can be used to eliminate the clutter return, thus increasing the probability of detection.

Assume that the sea surface consists of wave crests of nonuniform heights separated by water wavelength λ_w . If the scattering from these wave crests is nearly specular, the transient back-scattered electric field response will be a series of peaks separated in time by approximately $2\lambda_w \cos\theta_o/c$, where θ_o is the incidence angle measured from grazing incidence. Because this is analogous to the early-time response from a radar target, a frequency-domain E-pulse can be constructed to eliminate the sea clutter as a post-processing step. This enhances the ratio of energy in the signal to the energy in the clutter and improves the probability of detecting the target.

Under certain circumstances the clutter cancellation can also be accomplished in the time domain through direct transmission of an appropriate "clutter reducing transmit waveform" (CRTW). If the wave crests are fairly similar in height, the time domain scattered field response will be nearly periodic, and can be approximated by a sum of complex exponentials. It is then possible to create an E-pulse to eliminate the sea clutter directly in the time domain. Furthermore, it is possible to shape the E-pulse such that its energy is concentrated within the band of maximum target response (perhaps near the dominant target resonance) so that the radar return when this pulse is radiated contains both an enhanced target response and an eliminated clutter. Since this is not a post-processing step, both the target-to-clutter ratio and the signal-to-noise ratio are enhanced. If the E-pulse waveform is too complicated for direct transmission, a simplified version can be synthesized and transmitted using a superposition of short-pulse CW waveforms.

To simulate the potential of the time-domain approach, an aluminum missile model has been placed above a conducting aluminum sinusoidal surface, as shown in Figure 9, and illuminated by a horizontally-polarized EM wave. The backscattered field has been measured for an aspect angle of 30° from the horizontal in the frequency band 1-7 GHz both with and without the missile present. The resulting time-domain waveforms, obtained through Fourier inversion, are shown in Figure 10. As can be seen, the missile response is embedded within the strong clutter signal, and difficult to detect. To eliminate the clutter, a CRTW has been constructed using the clutter response, and convolved with the clutter + missile response to simulate its transmission. Figure 11 shows the result, indicating that the clutter has been reduced significantly, and the target response (appearing after about 2 ns) is easily detected.

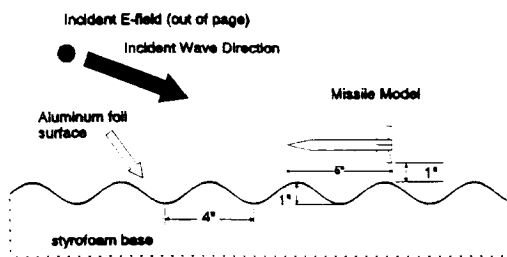


Figure 9. Simulated experimental sea surface environment.

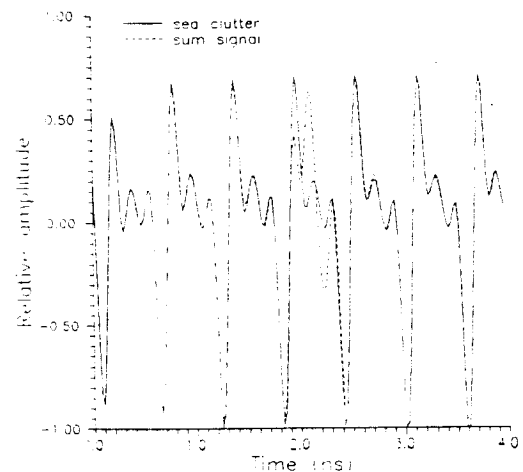


Figure 10. Measured response of simulated sea surface with and without 5 inch missile present.

In an actual application, it would not be known if the target was present, and thus the CRTW might be constructed using both target and clutter information. However, it is speculated that if the missile response is small, the resulting CRTW will eliminate the clutter without reducing the target response. To test this, a CRTW was created using the clutter + missile response of Figure 10 and convolved with the same response. The result, shown in Figure 12 demonstrates that while the clutter cancellation is not quite as good as when the CRTW was constructed from a pure clutter response, the missile response is still detectable over the clutter.

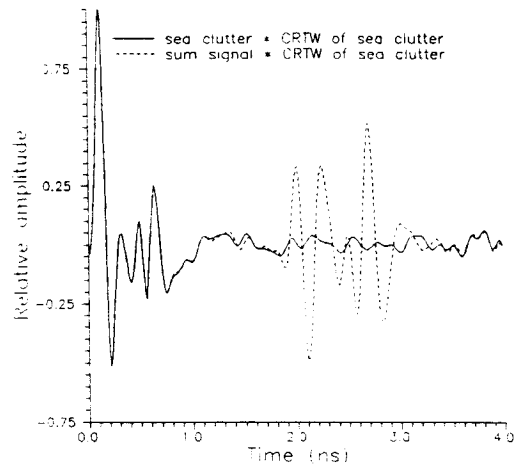


Figure 11. Convolution of measured response of sea surface with and without 5 inch missile with CRTW created from sea clutter response.

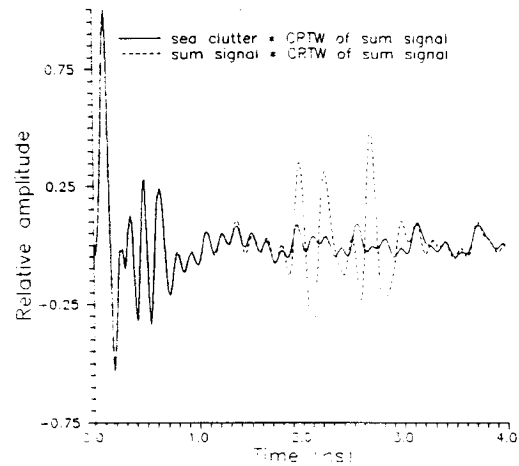


Figure 12. Convolution of measured response of sea surface with and without 5 inch missile with CRTW created from missile plus clutter response.

SEPARATION OF TARGETS FROM CLUTTER USING UWB/SP RADAR AND RELATIVE TARGET MOTION

A UWB/SP radar can be used to detect targets which move with different velocities than that of the ocean waves.

Consider a situation where a fast-moving target (e.g., a missile) and a stationary target (e.g., a periscope) are in the presence of a slow-moving ocean wave. If the sea surface is interrogated by a short EM pulse, the radar return will consist of a periodic series of peaks (the sea clutter from the ocean wave) and two peaks representing responses of the moving and stationary targets. When another interrogating pulse is sent out after a time interval, the new radar return will have a series of peaks shifted slightly due to the slow moving ocean wave, while the peak of the moving target will have moved a much larger amount, and the peak of the stationary target will not have moved. With repetitive interrogating pulses and each subsequent radar return recorded, a diagram such as shown in Figure 13 can be constructed. The horizontal axis is a fast time scale (ns) representing the location of targets and ocean wave crests. The vertical axis is a slow time scale (s) representing the time when the radar return is received. This diagram clearly shows the traces of moving and stationary targets and ocean wave crests. Using this relative motion scheme, targets can be separated from clutter, thus facilitating their detection.

This detection scheme was recently studied by the Naval Command, Control and Ocean Surveillance Center using actual measurements.

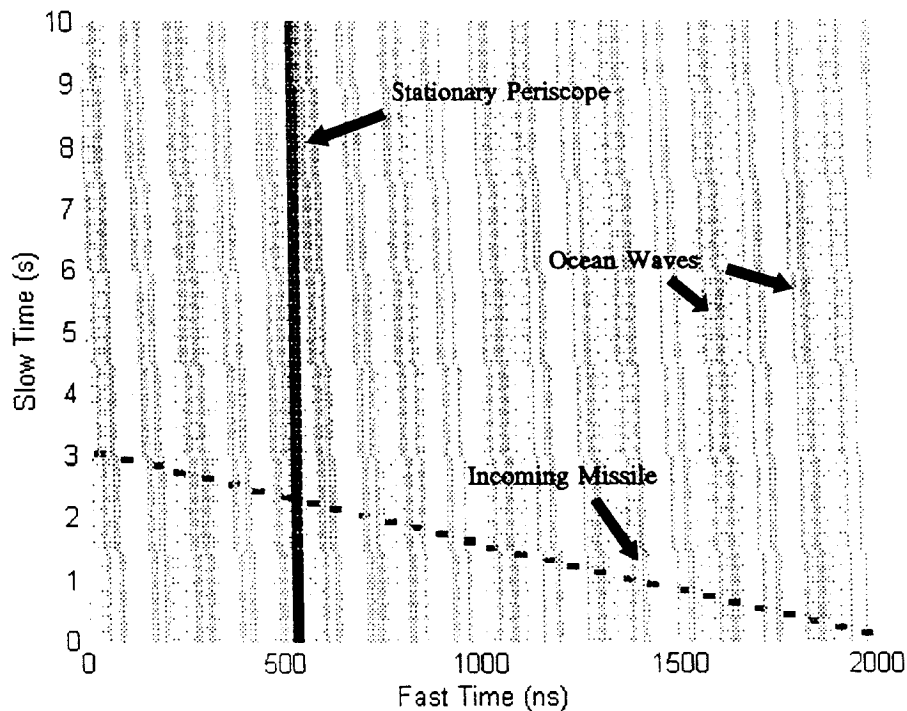


Figure 13. Traces of targets and ocean wave crests constructed using radar returns from repetitive interrogating EM pulses. Ocean wave velocity: 1 m/s, missile velocity: 100 m/s.

REFERENCES

1. E. Rothwell, K.M. Chen, D.P. Nyquist, P. Ilavarasan, J. Ross, R. Bebermeyer, and Q. Li, "Radar target identification and detection using short EM pulse and the E-pulse techniques", Ultra-Wideband, Short-Pulse Electromagnetics, Edited by H. Bertoni et al., Plenum Press, pp. 475-482, 1993.
2. J. Ross, P. Ilavarasan, E. Rothwell, R. Bebermeyer, K.M. Chen, D.P. Nyquist, and Q. Li, "Radar target discrimination using E-pulses with early-time and late-time responses", presented at 1993 IEEE-APS International Symposium/URSI Radio Science Meeting, June 28-July 2, 1993, University of Michigan, Ann Arbor, Michigan.
3. E. Rothwell, Q. Li, J. Ross, R. Bebermeyer, C.Y. Tsai, and K.M. Chen, "Non-Cooperative target recognition using ultra-wideband radars", Quarterly Report No. 5, Division of Engineering Research, Michigan State University, December 1993.
4. N.N. Bojarski, "A survey of the Physical Optics Inverse Scattering Identity," *IEEE Transactions on Antennas and Propagation*, vol. AP-30, No. 5, pp.980-989, September 1982.
5. W.H. Press, S.A. Teukolsky, W.T. Vetterling, and B.P. Flannery, Numerical Recipes in Fortran, 2nd ed., Cambridge University Press, 1992, chap. 13.
6. Tzi-Dar Chiueh and R.M. Goodman, "Recurrent Correlation Associative Memories," *IEEE Trans. Neural Networks*, vol. 2, pp. 275-284, March 1991.
7. Y. Kamp and M. Hasler, Recursive Neural Networks for Associative Memory, John Wiley & Sons, 1990.

ACKNOWLEDGEMENTS

The work was supported by Naval Command, Control and Ocean Surveillance Center under Contract N66001-91-C-6019, Office of Naval Research under Grant N00014-93-1-1272, and ThermoTrex Corporation under purchase order No. 22068.